



Top 15 musculoskeletal lesions in the aging recreational sporter: a pictorial review

Filip M. Vanhoenacker[^]

Department of Radiology, AZ Sint-Maarten Mechelen, University Hospital Antwerp, Ghent University, Mechelen, Belgium

Correspondence to: Filip M. Vanhoenacker. Department of Radiology, AZ Sint-Maarten Mechelen, University Hospital Antwerp, Ghent University, Liersesteenweg 435, Mechelen 2800, Belgium. Email: Filip.vanhoenacker@telenet.be.

Abstract: Because of the increased life expectancy, the aging population can participate in recreational sports activities. The fact that activity is promoted as having a positive effect on mental and physical health is another factor that may contribute to a trend of increased participation in sports activities by middle-aged and older patients. Due to age-related degeneration of tendons, muscles, joints and decreasing Bone Mineral Density, the musculoskeletal (MSK) system in the aging patient is more vulnerable to trauma. Therefore, sports-related lesions are commonly encountered in the daily routine of most imaging departments. In our radiological practice, we have seen a trend for an increase in sport-related injury referrals particularly in a population aged 40 years and over. Currently, 10% of referrals for imaging studies for sport injuries are in patients older than 40-year-old. This article consists of a pictorial review of the imaging appearance of the most encountered MSK lesions in aging recreational sporters in a radiological practice according to their anatomical location. We have chosen the 15 most encountered acute and overuse sports-related lesions involving the lower and upper extremity that are referred to our department of medical imaging. We especially focus on the most characteristic imaging findings on ultrasound and magnetic resonance imaging (MRI). Because of the high prevalence of MSK lesions in older asymptomatic patients, imaging findings must be interpreted in conjunction with the clinical presentation.

Keywords: Musculoskeletal imaging (MSK imaging); magnetic resonance imaging (MRI); radiology; ultrasound; sports injuries

Submitted Nov 22, 2022. Accepted for publication Apr 06, 2023. Published online Apr 14, 2023.

doi: 10.21037/qims-22-1294

View this article at: <https://dx.doi.org/10.21037/qims-22-1294>

Introduction

Today, sports activities are no longer the privilege of competitive and professional athletes. The democratization process made many sports disciplines, such as tennis, skiing, and golf amongst others accessible to a large population particularly in high income countries. This may lead to an increased participation of the aging population in sports activities (1). However, there is little evidence for a global change in sports participation among adults (2). To our

knowledge, there are no precise datasets on participation in sports in aging adults. With the ongoing increase in life expectancy—except for a decline in 2020 due to the COVID-19 pandemic (3) and the fact that cohort studies and randomized trials suggest that regular physical activity confers substantial health benefits (2,4), a large percentage of the aging population may get involved in recreational sports activities. In our radiological practice, in which approximately 35% of referrals for imaging concern musculoskeletal (MSK) studies, we have seen a trend for

[^] ORCID: 0000-0002-7253-1201.

an increase in sport-related injury referrals particularly in a population aged 40 and over. Currently 10% of referrals for imaging studies for sports injuries are in patients older than 40-year-old.

It may be hypothesized that due to age-related degeneration of tendons (5), muscles (6), and joints (7) as well as loss of bone strength resulting from osteoporosis (4,8), the MSK system in the aging population is more vulnerable to acute and/or repetitive trauma than in the young and well-trained sporting athletic population. This underscores the impact of sports medicine in our daily practice even in the general and aging population. Imaging plays an important role in the diagnosis and monitoring of sport-related injuries (9).

The aim of this article is to present a pictorial review of the imaging appearance of the most encountered MSK lesions in aging recreational sporters in our general radiological practice according to their anatomical location. Although the choice of the reported lesions may seem to be a bit arbitrary, it reflects the occurrence of the most common sports related injuries in our radiological practice.

Conventional radiography was performed on the Luminos dRF MAX (Siemens, Erlangen, Germany). US images using EPIQ5G (Philips Health Systems, Bothell, WA 98021, USA) or RS85 Prestige (Samsung Healthcare, Seoul, South Korea), magnetic resonance (MR) examinations were performed on a 1.5T system (Siemens, Magnetom Aera or Magnetom SolaFit, Erlangen, Germany). MR protocols for MSK imaging are provided as [Tables S1-S7](#).

Lower extremity

Hamstrings rupture

The hamstrings consist of 3 muscles including the biceps femoris, semitendinosus, and semimembranosus, crossing the hip and knee (10). These muscles coordinate hip extension with a flexed knee. The biceps femoris and semitendinosus have a common tendinous insertion at the posteriorly located transverse facet of the ischial tuberosity, whereas the semimembranosus tendon inserts more anteriorly at the oblique facet of the ischial tuberosity (10,11).

The spectrum of proximal hamstring tendon injuries ranges from proximal tendinopathy to partial tears to complete avulsions (12). An avulsion injury occurs when the bone tears completely away from the ischial tuberosity. Avulsions may occur due to a sudden eccentric muscle

contraction with an extended knee and a flexed hip, often in a weakened tendon due to preexisting hamstrings tendinopathy. Hamstrings tears can occur in a variety of sports most commonly water skiing in younger patients, and tennis, badminton, volleyball, soccer, and golf in older recreational sporters (13).

Patients may present with sudden pain, focal swelling due to retraction or even neuropathic pain due to swelling and edema of the adjacent sciatic nerve. Ultrasound (US) may be difficult because of the relative deep location of the hamstrings tendons especially in obese patients. Therefore, magnetic resonance imaging (MRI) is the imaging modality of choice compared to US to assess whether the lesion is partial or complete and to assess the degree of tendon retraction and residual tendon quality (*Figure 1*) (13).

Meniscus tear

The knee is probably the most frequently involved joint in the aging sporter, with injuries of the meniscus being the predominant lesion often in conjunction with cartilage and ligamentous damage. Meniscus tears are most frequently seen in recreational soccer players and skiers. The type of meniscal tear can range from longitudinally oriented (either vertical or horizontal), to radial or root tears. A complex tear consists of a combination of these basic types (*Figure 2*) (14). Radial and root tears may cause meniscus extrusion. A displaced tear may cause joint locking. Surgical treatment of meniscal tears can be broadly divided into those in which partial meniscectomy or meniscal repair are performed. Meniscal repair is performed exclusively on younger populations, while older populations are subject to partial meniscectomy procedures because the meniscus is less amenable to repair in older patients (15). Not all meniscal tears need arthroscopic treatment, particularly in the aging patient. Indeed, atraumatic meniscal tears are frequently encountered on MRI in the older population with coexisting cartilage loss. In this scenario, there is lack of supporting evidence that arthroscopic treatment is superior to conservative treatment consisting of weight loss and exercise therapy (15-18). The exception to this rule may be when mechanical symptoms, such as knee locking occur (15).

Anterior cruciate ligament (ACL) lesion

Lesions of the ACLs are also very commonly seen in the aging sporters such as skiers and soccer players, often in

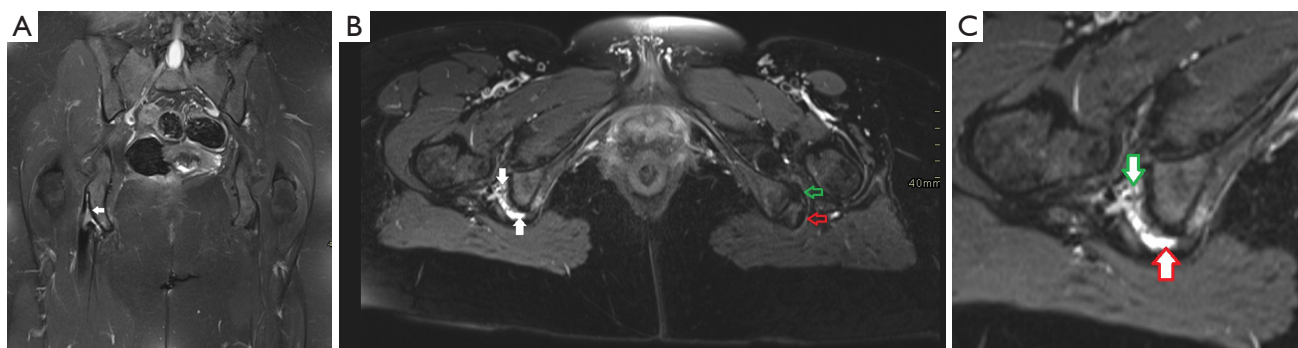


Figure 1 Almost complete avulsion of the right hamstrings in a 51-year-old female presenting with acute pain during golf. (A) Coronal FS T2-WI showing complete avulsion of the right conjoint tendon (white arrow). There is minor residual remnant of the superolateral aspect of proximal attachment of the semimembranosus tendon. (B) Axial FS T2-WI showing absence of the proximal hamstring tendons (white arrows) on the right side compared to the left side. Note the normal hypointense aspect of the semimembranosus tendon (open green arrow) anteriorly and the conjoint tendon (open red arrow) on the left side. (C) Enlarged axial FS T2-WI of the right side demonstrates a fluid-filled gap between the ischial tuberosity and the semimembranosus tendon (anterior open green arrow) and between the ischial tuberosity and the conjoint tendon (posterior open red arrow). FS, fat suppressed; WI, weighted image.

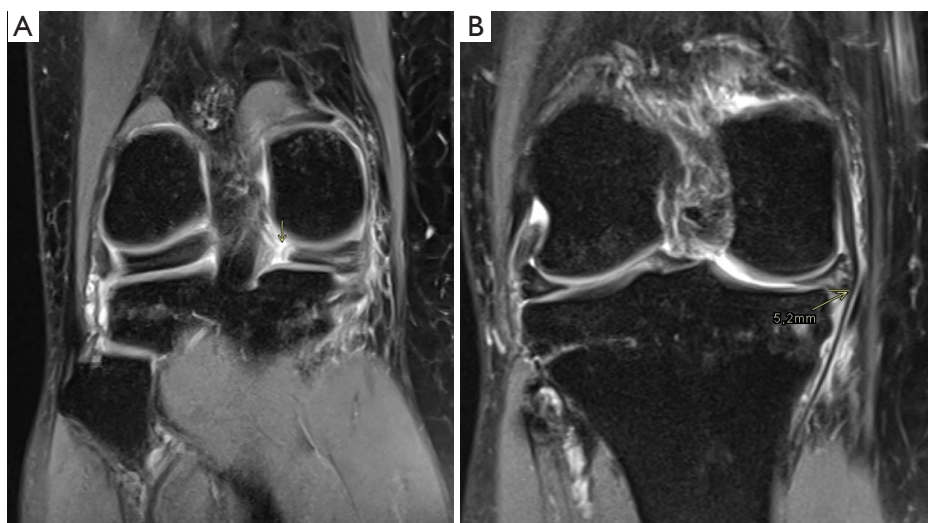


Figure 2 Complex medial meniscus tear in a 52-year-old male skier. (A) Coronal FS T2-WI at the posterior horn and (B) coronal FS T2-WI at the corpus of the medial meniscus of the right knee. There is a horizontal tear of the posterior and corpus of the medial meniscus and a radial tear at the intercondylar part of the posterior horn (arrow in A) and an extrusion of the corpus relative to the medial tibia (B). The high signal in the meniscus tear is due to joint fluid filling the meniscus defect. FS, fat suppressed; WI, weighted image.

association with meniscal and other ligamentous lesions, depending on the mechanism of trauma (19). The imaging semiology on MRI is not different from ACL lesions in the young competitive athlete and consists of direct signs of tear (ligamentous discontinuity) and indirect signs (bone marrow edema at the posterolateral tibia and the middle portion of the lateral femur condyle) (*Figure 3*).

Subchondral insufficiency fracture (SIF)

SIF occurs as a consequence of mechanical failure of the subchondral cancellous bone (20). SIF may be seen in aging recreational sporter due to overuse with abnormal transarticular load distribution e.g., occurring after partial meniscectomy and radial or root tears of the meniscus (21).

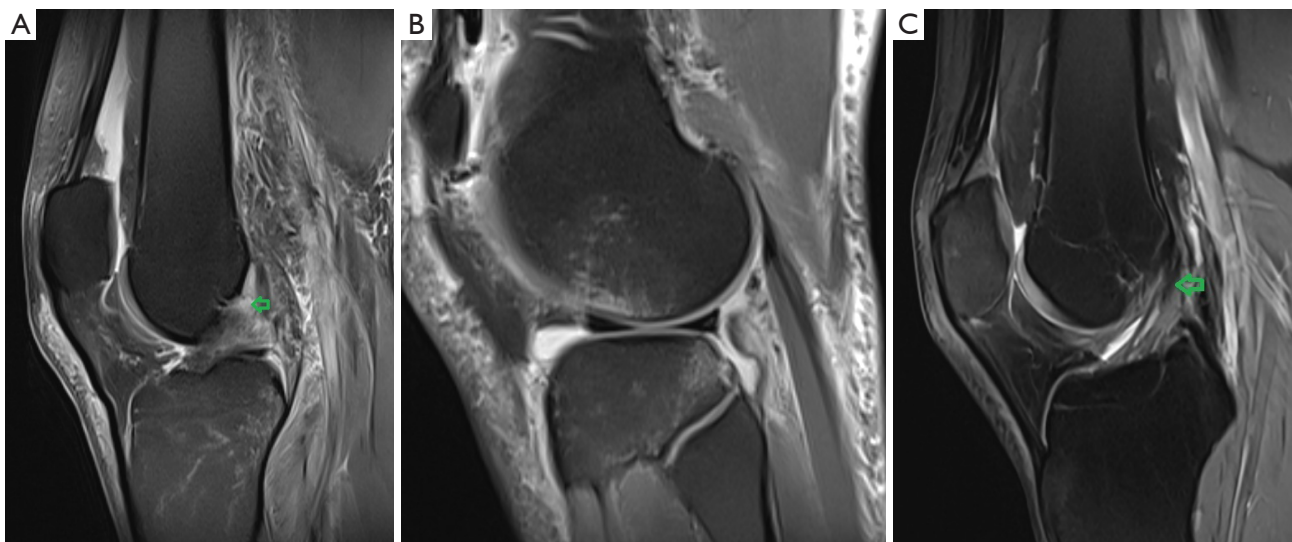


Figure 3 Complete ACL tear a 40-year-old male skier. (A) Midsagittal FS T2-WI shows discontinuity of the femoral portion of the ACL (green open arrow). (B) Sagittal FS T2-WI at lateral compartment shows bone marrow edema at the posterolateral tibia and the middle portion of the lateral femur condyle due to anterior translation of the tibia and impaction of the posterolateral tibia and the lateral femur condyle. (C) Midsagittal FS T2-WI shows a hypointense signal of the femoral portion of a normal ACL (green open arrow) for comparison. The striated aspect of the tibial portion of the ACL is a normal finding. ACL, anterior cruciate ligaments; FS, fat suppressed; WI, weighted image.

Particularly in females, there may be preexisting osteoporosis (22), although this has been questioned (23). Overweight is another risk factor (20).

The lesion is typically seen at the joint of the lower extremity including the hip, knee and ankle. Plain radiographs are usually unremarkable. On MRI, the fracture line is hypointense on both pulse sequences and typically parallels the subchondral bone plate without disrupting it. The fracture line is difficult to distinguish between the two layers of the subchondral plate on fluid-sensitive sequences, and a single linear low-signal band is better recognized on T2-weighted image (T2-WI) or proton density-weighted image (PD-WI) (22,24). The overlying cartilage is intact. The fracture is surrounded by extensive bone marrow edema (25) (*Figure 4*).

If nontreated appropriately by restriction of weight-bearing, SIF may lead to subchondral collapse, secondary osteonecrosis and destructive arthropathy (20).

Stress fracture

Stress fracture consists of failure of bone due to repetitive microtrauma, often seen in aging sporters with insufficient training (20). There are 2 subtypes of stress fractures,

i.e., fatigue fractures due to overuse in a normal bone and insufficiency fracture occurring in weakened bone. Plain radiographs are often negative in the first weeks after the onset of pain.

On MRI, cortical stress fracture is associated with adjacent periosteal and endosteal edema. Trabecular stress fracture are oriented perpendicular to compressive trabeculae and surrounded by bone marrow edema (*Figure 5A-5C*) (20).

Bone scintigraphy shows a focal area of increased tracer uptake (*Figure 5D*). Bone scintigraphy typically uses intravenous injection of ^{99m}m-labelled phosphates or diphosphonates. These agents bind to hydroxyapatite crystals in bone, in proportion to osteoblastic activity and blood flow (8).

Tennis leg

Tennis leg refers to a tear of the myotendinous junction of the medial head of the gastrocnemius, which is typically seen in middle-aged tennis players but may be seen in other sports causing sudden forced dorsiflexion of the ankle while the knee being in extension such as badminton, squash, padel, skiing, running, athletics, hurdling, jumping (26,27).

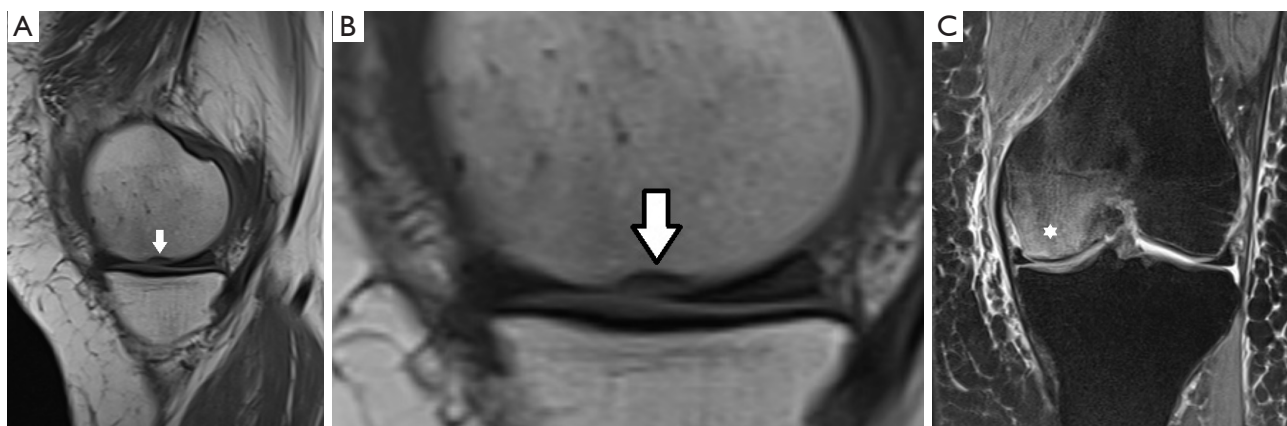


Figure 4 Subchondral insufficiency fracture of the medial femoral condyle of the left knee in a 60-year-old female following long distance walking. (A) Sagittal T1-WI showing a hypointense fracture line paralleling the subchondral bone plate (white arrow). (B) Enlarged sagittal T1-WI showing a hypointense fracture line paralleling the subchondral bone plate (arrow). (C) Coronal FS T2-WI shows extensive surrounding bone marrow edema in the medial femoral condyle (white asterisk). The overlying articular cartilage is intact. FS, fat suppressed; WI, weighted image.

Patients presents with sudden snapping and sharp pain within the posterior calf, with focal tenderness and swelling or palpable focal gap at the site of the tear (27).

US shows fluid deep to the myotendinous junction of the medial gastrocnemius and superficial to the soleus muscle with disruption in contour and echogenicity of muscle fibers of the distal medial gastrocnemius (*Figure 6*) (27). Involvement of the plantaris tendon is uncommon (27,28).

MRI demonstrates a focal area of disruption of muscle continuity along the deep aspect of the medial head of the gastrocnemius, with associated muscle edema and fluid deep to medial gastrocnemius and superficial to the soleus (*Figure 7*) (28).

Achilles tendon tear

Tears almost always occur in an already diseased tendon. Achilles tendon tears results from a sudden contraction of the gastrocnemius and soleus muscles. Achilles tendon tears are often seen in middle-aged patients with pre-existing Achilles tendinopathy particularly in sports as tennis, badminton, padel, football or basketball (26). Corticosteroid injection is another cause of Achilles tendon tear. Corticosteroids inhibit production of extracellular matrix collagen, which may result in a degenerative process reducing the strength and elasticity of the tendon. Together

with the poor local vascularization of the distal Achilles tendon, this may cause partial rupture and subsequent complete rupture of the tendon (29).

Symptoms include acute pain and swelling and the inability to walk. Tears are either partial or complete and localised at the hypovascular midportion of the tendon, about 6cm proximal to the insertion, or at the myotendinous junction. Plantar flexion of the foot may be preserved when the plantaris tendon is still intact (30,31).

US is the preferred imaging modality to confirm the clinical diagnosis of a complete tear (32). The size of the anechoic tendon gap increases with the foot in dorsiflexion (*Figure 8*). Herniation of the adjacent fat pad can also be present. Torn ends of the tendon on each side of the gap are best demonstrated on longitudinal panoramic views (*Figure 8*). A focal hypoechoic area with loss of fibrillation parallel to the tendon fibres is seen in a partial tear.

MRI is helpful especially in cases where US is equivocal. Complete tears are identified by discontinuity of the tendon with a fluid-fluid gap interposed between the torn ends. MRI is also useful to demonstrate secondary muscle atrophy and fatty infiltration in the calf muscles after Achilles tendon repair (33). A partial tear on MRI demonstrates a heterogeneous increased signal on fluid-sensitive images and partial disruption of the tendon fibres (30,31,34,35).



Figure 5 Stress fracture of the left distal tibia in a middle-aged female runner, presenting with pain during a start-to-run program. (A) Coronal T1-WI of the ankle showing an oblique hypointense fracture line within the cancellous bone extending to the medial cortex of the tibia and subtle surrounding periosteal reaction (arrow). (B) Detailed coronal T1-WI shows better the fracture line (open green arrow). (C) Axial FS T2-WI shows a subtle hyperintense fracture line in the medial cortex of the tibia with adjacent bone marrow edema and periosteal edema (arrow). (D) Bone scintigraphy reveals increased tracer uptake in the left distal tibia. WI, weighted image; FS, fat suppressed.

Snowboard fracture of the ankle

Although ligamentous ankle sprain is one of the most common MSK traumatic lesions, this is not specifically seen in the sporting population and therefore detailed discussion is omitted in this article.

A snowboard fracture is a more specific sport-related fracture of the lateral process of the ankle due to dorsiflexion and inversion of the ankle, which typically

occurs in snowboarding but may be seen in other winter sports (36). Clinically, there is soft tissue swelling distal to the lateral malleolus and it may mimic lateral ankle sprain.

The fracture is often missed on conventional radiographs due to superimposition of adjacent bony structures (37). Therefore, CT and/or MRI (*Figure 9*) are the preferred imaging tools for detection and evaluation of the extent and degree of displacement of fracture fragments (38).

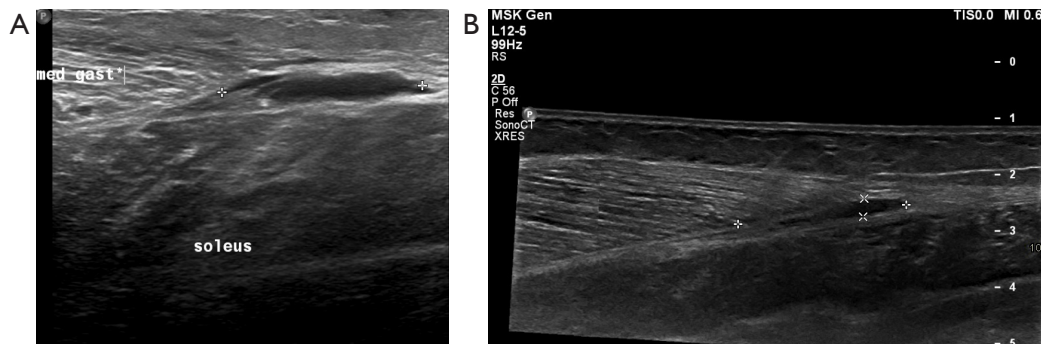


Figure 6 Tennis leg of the right calf in a 61-year-old tennis player. (A) Longitudinal US and (B) panoramic view shows an anechoic fluid collection deep to the medial gastrocnemius and superficial to the soleus muscle. There is disruption of the muscle fibers of the distal medial gastrocnemius. US, ultrasound.

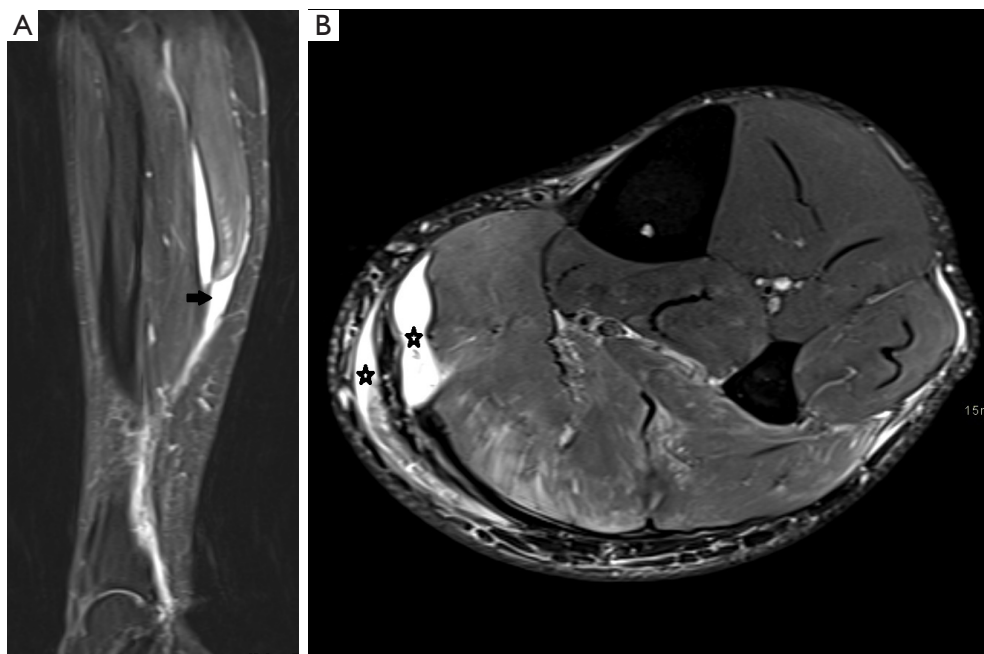


Figure 7 Tennis leg of the right calf in a 52-year-old badminton player presenting with a sudden painful snap in the left calf. (A) Sagittal FS T2-WI reveals a hyperintense fluid collection between the medial head of the gastrocnemius and soleus. Note retraction of the distal gastrocnemius (black arrow). (B) Axial FS T2-WI shows a hyperintense fluid collection adjacent to the distal medial gastrocnemius (stars). There is also feathery oedema in the gastrocnemius and soleus muscles. FS, fat suppressed; WI, weighted image.

Morel-Lavallée lesion (MLL)

MLL consists of a serosanguineous collection separating the skin and subcutaneous fat from the underlying fascia. MLL results from a degloving injury causing sudden shearing forces occurring tangential to the fascial planes, causing the more mobile dermis and subcutaneous fat to abruptly move relative to the firmer underlying fascia. The lesion

has a predilection for certain locations such as the greater trochanter/hip followed by the thigh and the pelvis and knee. The lesion may—however—be seen anywhere in the body.

MLL is typically seen after a fall with a motorbike, but may be seen in recreational cyclists, particularly those using an e-bike, causing a higher velocity trauma. Patients present



Figure 8 Complete achilles tendon tear in a 52-year-old female badminton player presenting with a sudden painful snap in the left calf. (A) Longitudinal ultrasound with plantar flexion of the foot shows an anechoic gap in the achilles tendon. (B) On a longitudinal ultrasound with dorsiflexion of the foot, the size of the gap increases. (C) Panoramic longitudinal view shows better the proximal and distal tendon gap. (D) Partial Achilles tendon tear in another 67-year-old male. Sagittal FS T2-WI reveals an intratendinous focus of high signal (green arrow). There is pre-existent tendinosis with fusiform swelling of the Achilles tendon. Note also linear high signal adjacent to the anterior and posterior aspect of the tendon indicating paratenonitis (red arrows). FS, fat suppressed; WI, weighted image.

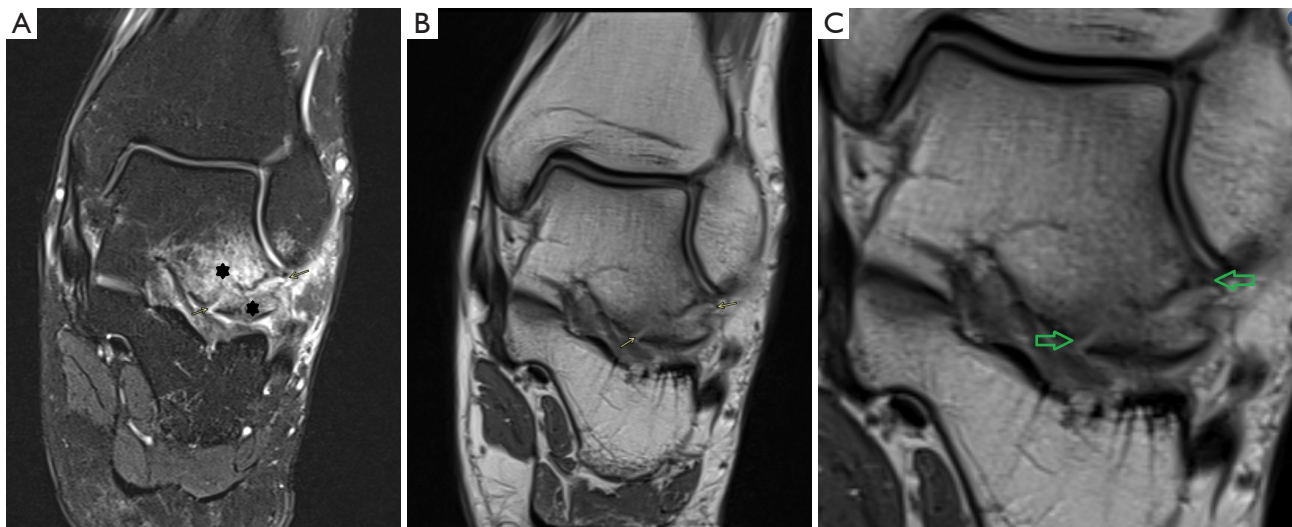


Figure 9 Snowboard fracture in a middle-aged snowboarder. (A) Coronal FS T2-WI shows bone marrow edema at the lateral process of the talus (asterisks). (B) Coronal Proton density image without fat suppression shows a hypointense fracture line at the lateral process of the talus (arrows). (C) Magnification view of the coronal proton density image without fat suppression shows better the fracture line (green arrows). FS, fat suppressed; WI, weighted image.

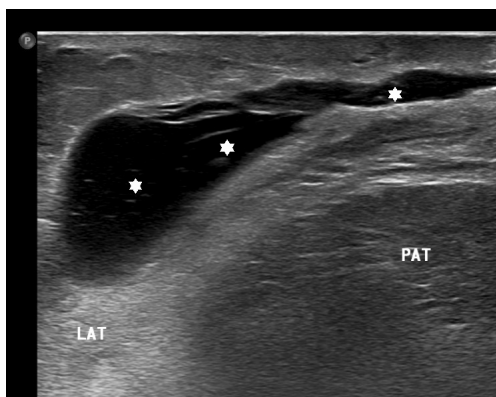


Figure 10 Morel-Lavallée lesion in a 77-year-old recreational female cyclist presenting with a compressible prepatellar soft tissue swelling following a fall. Axial ultrasound shows an anechoic collection with subtle intralesional septations (asterisks) separating the subcutaneous fat and the patellar retinaculum. LAT, lateral; PAT, patella.

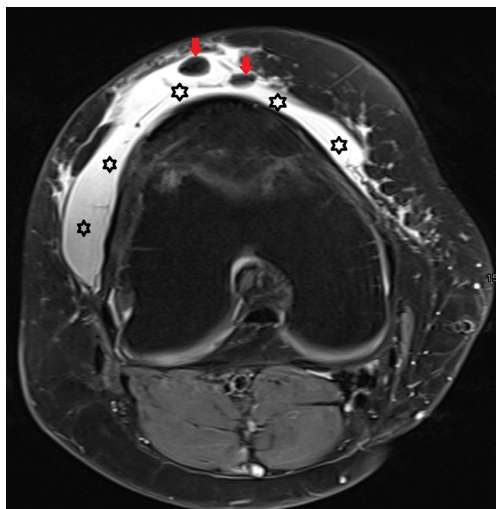


Figure 11 Morel-Lavallée lesion in another 62-year-old recreational female cyclist presenting with a soft tissue swelling at the knee following a fall. Typically, Morel-Lavallée lesion at the knee joints extends more medially and laterally along with the patellar retinacula, compared to a prepatellar bursa which has a median location. Axial FS T2-WI shows a fluid-filled collection separating the subcutaneous fat and the patellar retinacula (asterisks). Small areas of isointense signal to fat consistent with the presence of fat globules are seen anteriorly in the collection (red arrows). FS, fat suppressed; WI, weighted image.

with pain and swelling in the affected area and physical examination reveals a soft fluctuant mass with contour deformity.

US typically shows a fusiform or oval anechoic or hypoechoic lesion. It is compressible with the US transducer. Intralesional fat globules may be seen as small hyperechoic foci. Some lesions may contain internal septations or a fluid-fluid level (*Figure 10*).

MRI may be used for a global overview of the lesion's extent, particularly in large lesions. The signal of the lesion may vary along with the intralesional blood degradation products. In most scenarios, the signal is hypointense or slightly hyperintense on T1-WI and hyperintense on T2-WI. Intralesional fluid-fluid levels, septations or fat globules may be present (39) (*Figure 11*).

Morton's fibroma

Morton's fibroma consists of a perineural thickening surrounding the digital nerve of the foot typically occurring at the third web space and more rarely at the second web space, usually in response to irritation, trauma, or excessive pressure. Although Morton's fibroma is often designated as an interdigital neuroma, this is a misnomer as the lesion does not represent a true neuroma but a pseudotumoral reactive fibrous lesion around the interdigital nerve (40).

Morton's fibroma is much more common in women than men and typically affects middle-aged patients and is often seen in recreational walkers and runners. Patients present with burning or sharp pain in the ball of the foot irradiating to the toes sometimes with associated numbness in the toes. Some patients feel that they walk on a marble.

At physical examination, the Mulder sign may be seen consisting of a painful click which can be reproduced by squeezing the two metatarsal heads together with one hand, while concomitantly putting pressure on the interdigital space with the other hand.

US shows a well-defined and non compressible hypoechoic lesion in the intermetatarsal space proximal to the metatarsal head (41). The Mulder sign may be elicited with the US transducer as well (42). To perform Mulder's test during sonography, the patient should lie prone with the feet resting on the examining table. The examiner's

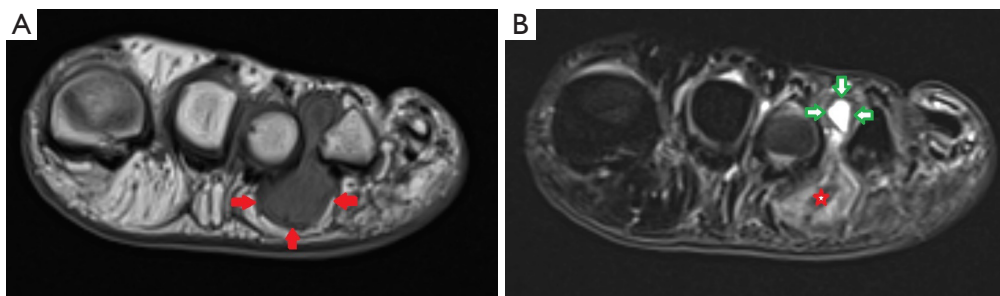


Figure 12 Morton's fibroma in a 49-year-old female long-distance walker. (A) Short axis T1-WI shows an hour-glass shaped lesion in the third web space (red arrows). (B) On short axis FS T2-WI, the lesion is a mixed signal intensity with hypointense and intermediate signal (red asterisk). There is associated fluid (green arrows) within the intermetatarsal bursa. WI, weighted image; FS, fat suppressed.

nonimaging hand firmly grasps the foot at the level of metatarsal heads. The transducer is positioned in a coronal plane to the plantar aspect of the intermetatarsal region to localize the Morton's fibroma between the metatarsal heads. By squeezing the metatarsals together while relieving pressure on the transducer, the Morton's fibroma—if present—may displace toward the plantar surface, and a painful click may be felt (42).

The presence of continuity with the plantar digital nerve can improve diagnostic confidence (40). On MRI, the lesion is most often isointense to muscle on T1-WI and hypointense to mixed on T2-WI. The enhancement is variable (43). There may be associated fluid in the intermetatarsal bursa (*Figure 12*).

Upper extremity

Rotator cuff tear

Rotator cuff tear is a very common source of shoulder pain and disability in daily practice. Typically, rotator cuff tears occur more frequently in elderly than in younger patients, following a chronic or acute-on-chronic course with preexisting tendon degeneration (44). US is a well-established and cost effective technique for evaluation of rotator cuff tendinopathy, subacromial-subdeltoid bursitis and rotator cuff tear (*Figure 13*) (45).

MRI can more accurately evaluate the size and shape of tendon tears, degree of tendon tear retraction, and tendon and muscle quality (45). MR arthrography is more sensitive than plain MRI for the diagnosis of articular-sided partial-thickness rotator cuff tears (*Figure 13*) (46).

Distal clavicular osteolysis

Distal clavicular osteolysis consists of an isolated osteolysis of the acromial end of the clavicle due to either chronic repetitive stress or less commonly a single acromioclavicular trauma. It is not clear why the changes predominate in the clavicle with relative sparing of the acromion (47).

Weightlifters, bodybuilders and other overhead sporters are at risk (48,49). Clinical findings are often nonspecific. There is focal tenderness over the acromioclavicular joint (AC-joint) and painful cross-body adduction (49). Radiographic changes include cortical thinning, irregularity, microcysts in distal clavicle and mild AC-joint widening (47). Tapering may be seen in advanced stages (49) (*Figure 14*). US shows irregular delineation of the lateral clavicle and joint effusion (*Figure 15*).

MRI is more sensitive than radiography for early detection. MRI shows typically bone marrow edema in the distal clavicle, sometimes also to a minor degree in the articular part of the acromion (47). Other findings include subchondral fracture of the clavicle, widening of the acromioclavicular with joint effusion, intra-articular bone fragments and capsule hypertrophy (*Figure 16*) (47).

Biceps brachii tendon rupture

Rupture of the distal brachii occur in middle-aged male with a peak at around 50 years of age (50). Bodybuilders particularly those using anabolic steroids are at risk (50).

Patients typically present with a history of marked pain on eccentric loading accompanied by a popping sound. Subsequent symptoms are pain, bruising at the

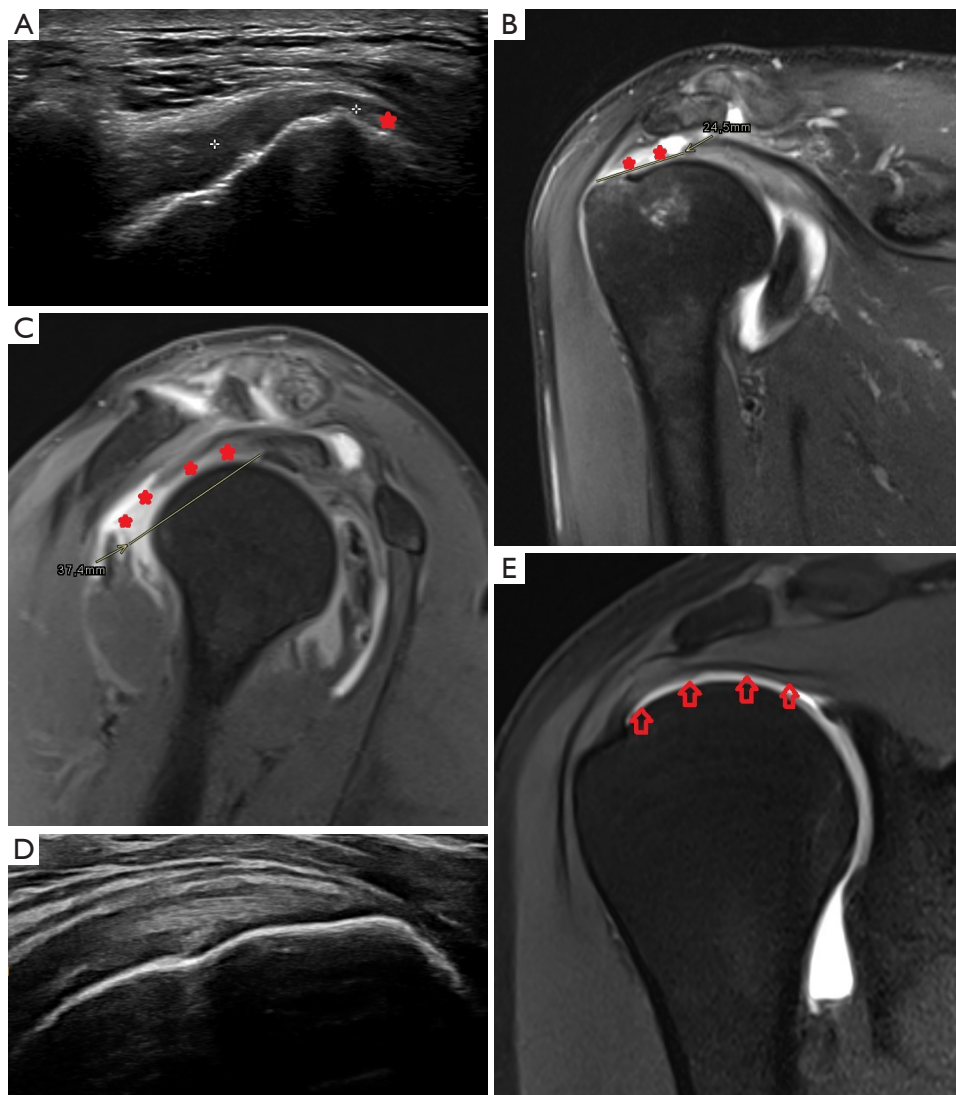


Figure 13 Traumatic rotator cuff tear in a 55-year-old male presenting with a painful shoulder and loss of muscle strength following bench pressing. (A) Longitudinal US loss a fibrillar structure (compare to panel D) of the supraspinatus tendon. Note instead an area of structureless heterogeneous echotexture adjacent to the greater tuberosity (between callipers). There is fluid and debris within the subacromial bursa adjacent to the greater tuberosity (red asterisk). These findings are highly suspicious for a full-thickness rotator cuff tear. (B) Oblique coronal and (C) oblique sagittal MR arthrogram shows leakage of contrast into a gap within the supraspinatus and infraspinatus tendon (red asterisks). MR arthrography is superior to US to demonstrate the size, extent (supraspinatus and infraspinatus are involved in this case) and degree of retraction of the tear. There is also communication of the full-thickness tear with the acromioclavicular joint which is a negative prognostic parameter for surgical repair. (D) Longitudinal US in a volunteer showing a normal fibrillar structure of the supraspinatus tendon. (E) Oblique sagittal MR arthrogram shows a normal delineation of the articular side of the supraspinatus in another patient (red arrows). MR, magnetic resonance; US, ultrasound.

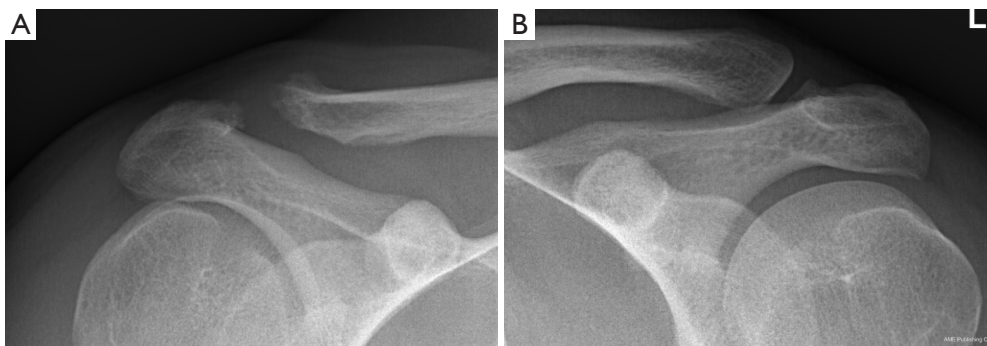


Figure 14 Distal clavicular osteolysis at the right clavicle in a middle-aged weightlifter. (A) Radiograph of the right AC joint shows irregular delineation and tapering of the right clavicle and widening of the AC joint. (B) Normal radiograph of the left AC joint for comparison. AC, acromioclavicular.

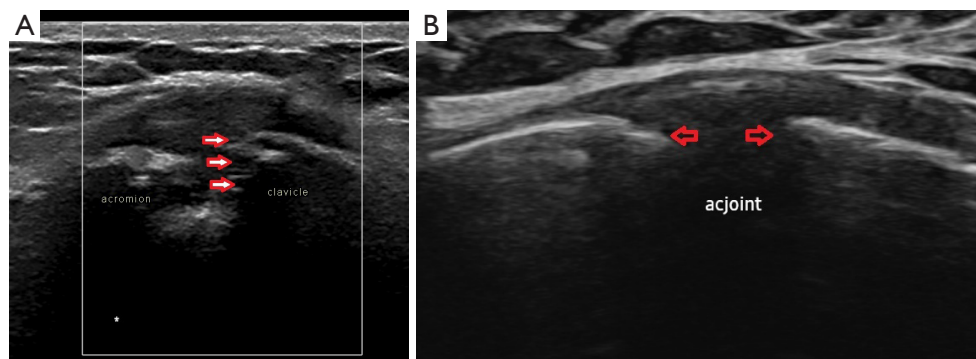


Figure 15 Distal clavicular osteolysis at the right clavicle in a 49-year-old weightlifter. (A) Ultrasound of the right AC joint shows irregular delineation of the right clavicle (red arrows), joint effusion and widening of the AC joint. (B) Ultrasound of a normal right AC joint for comparison. Note regular delineation of the articular side of the acromion and clavicle (red arrows). AC, acromioclavicular.

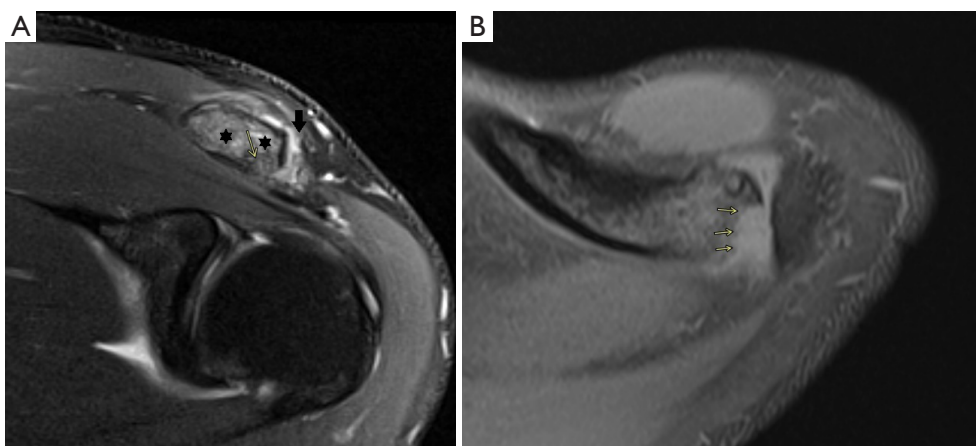


Figure 16 Distal clavicular osteolysis at the left clavicle in middle-aged body builder. (A) Coronal FS T2-WI shows bone marrow edema at the clavicle (asterisks), joint effusion (thick black arrow) and widening of the AC joint and focal irregular delineation of the lateral clavicle (small arrow). (B) Axial FS-T1-WI better shows the irregular delineation of the lateral clavicle (small arrows). Note also a small subchondral cyst anteriorly. FS, fat suppressed; WI, weighted image; AC, acromioclavicular.

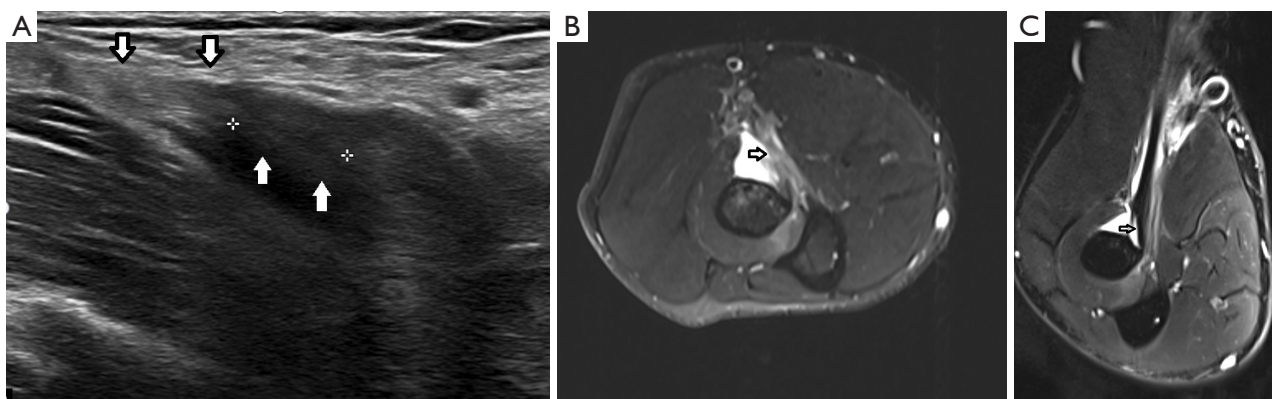


Figure 17 Partial tear of the long head of the distal biceps brachii in a 53-year-old recreational javelin thrower. (A) Longitudinal ultrasound showing irregular delineation of the deep portion of the long head of the biceps brachii (white arrows). There is still continuity of the superficial part and the short head (white arrow with black contour). There is fluid surrounding the distal biceps tendon. (B) Axial FS-T2-WI and (C) coronal FS-T2-WI in FABS position shows irregular delineation and thinning of the long head of the biceps brachii (white arrows with black contour). Note fluid adjacent to the distal biceps tendon. FS, fat suppressed; WI, weighted image; FABS, Flexed, shoulder ABducted and forearm Supinated.

antecubital fossa and weakness in elbow flexion and/or forearm supination (50). Clinical examination may reveal an abnormal contour of the distal biceps (50). Tears may be either partial or complete. US may demonstrate partial (Figure 17) or complete tendon discontinuity (Figure 18) with peritendinous effusion, with or without tendon retraction depending on whether the lacertus fibrosus is intact or discontinuous. As the biceps brachii changes direction distally, US is often hampered by anisotropy artefact. Moreover, it is difficult to assess intactness of the lacertus fibrosus which is a thin structure.

Various approaches for optimal sonographic assessment of the distal biceps tendon have been suggested in the literature: the anterior, lateral, medial and posterior approach (51).

The anterior approach with longitudinal orientation of the US transducer can be challenging because the steep oblique course and 90° of rotation of the tendon may result in anisotropy mimicking tendinosis or tear (52,53).

To avoid anisotropy, the US transducer can be positioned slightly inferolaterally in order to maintain the transducer parallel to the tendon as it courses obliquely away from the probe to its insertion (53). Other tricks that may help to avoid misinterpretation of anisotropy as tendinosis or a tear are application of more pressure on the distal half of the transducer (“heel-toe maneuver”) and the use of various degrees of elbow flexion and extension (53).

The lateral approach uses the supinator and

brachioradialis muscle as window with the elbow flexed and the forearm in maximal pronation and the wrist flexed. The medial approach uses the pronator muscle as window with the elbow flexed in 20° to 30° and the forearm in supination. Finally, the posterior approach uses the anconeus as window (51).

On MRI (Figure 17B,17C, Figure 18B-18D), it is pivotal to cover the whole distal biceps tendon from the musculotendinous junction to its distal insertion at the radial tuberosity. In addition to axial and sagittal images, it is recommended to use coronal images with elbow Flexed, shoulder ABducted and forearm Supinated (FABS) position to improve visualization of the distal biceps brachii insertion (54).

MRI aims to evaluate whether the tear is partial or complete, involves the long and/or short head of the biceps and the integrity of the lacertus fibrosus and the degree of tendon retraction. Tears are often associated with fluid around the distal biceps tendon or bicipitoradial bursitis (55).

Tennis/golfers elbow

Lateral epicondylitis, also known as tennis elbow, is an overuse syndrome of the common extensor tendon. The extensor carpi radialis brevis (ECRB) tendon is most affected. Patients present with lateral elbow pain, tenderness and swelling. Radiographs may normal but may show calcifications adjacent to the lateral epicondyle and irregular delineation of the lateral epicondyle.

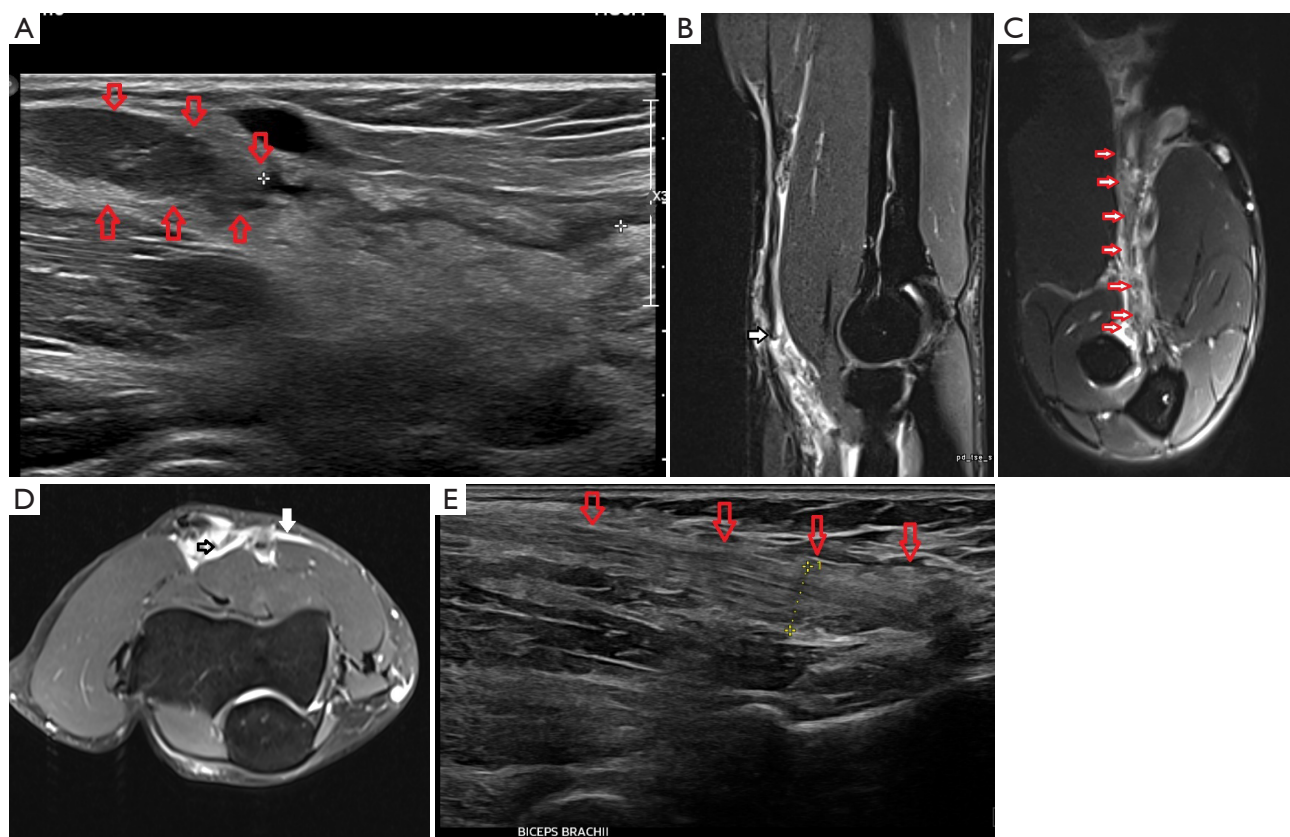


Figure 18 Complete tear of the long head of the distal biceps brachii in a 50-year-old male presenting with a sudden popping sensation during bench pressing. (A) Longitudinal ultrasound showing complete discontinuity and proximal retraction of the biceps brachii (red arrows showing retracted tendon stump). (B) Sagittal and (C) Coronal FS-T2-WI in FABS position shows discontinuity and proximal retraction of the biceps brachii (arrows). (D) Axial FS-T2-WI shows discontinuity of the biceps tendon (white arrow with black contour) and lacertus fibrosus (white arrow). The latter is responsible for tendon retraction. (E) Longitudinal ultrasound showing normal continuity and fibrillar structure of the biceps brachii (red arrows) in a normal individual for comparison with panel A. FS, fat suppressed; WI, weighted image; FABS, Flexed, shoulder ABducted and forearm Supinated.

US may confirm calcifications and irregularity of the lateral epicondyle. In case of tendinopathy, the extensor tendon is usually thickened, hypoechogenic and may show hyperemia on color Doppler (*Figure 19*) (56). MRI shows thickening and increased signal intensity on FS T2-WI within the common extensor origin sometimes with associated peritendinous and bone marrow edema (57).

Partial or more rarely complete tear are seen as fluid-filled gaps in the extensor tendons on US or MRI (*Figure 20*). The radial collateral ligament may be ruptured as well (57). *Medial epicondylitis*, also known as golfers' elbow, is less frequent and the medial counterpart of tennis elbow involving the flexor tendons. The imaging semiology is similar to lateral epicondylitis (57).

Ulnar collateral ligament (UCL) lesions of the thumb and stener lesion

Avulsion or rupture of the UCL of the first metacarpophalangeal joint is also known as Gamekeeper's thumb or skier's thumb. Gamekeeper's thumb refers to a chronic overuse of the UCL ultimately leading to tearing, whereas skier's thumb represents an acute injury of the UCL due to sudden forceful thumb abduction when the thumb is caught in the strap of the ski pole during skiing (20). The lesion is commonly encountered in recreational middle-aged skiers.

UCL lesion is usually located at the distal insertion at the proximal phalanx of the thumb and may include either partial, complete or avulsion fracture. A Stener lesion consists of proximal retraction of the ruptured UCL with

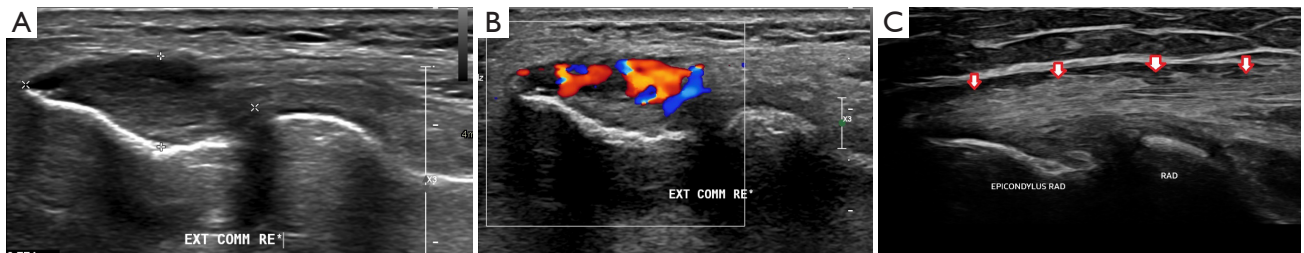


Figure 19 Tennis elbow with proximal extensor tendinopathy in a middle-aged tennis player. (A) Longitudinal gray scale ultrasound showing thickening and hypoechoogenicity of the proximal extensor tendon. (B) Longitudinal ultrasound with power doppler shows hypervascularity of the affected tendon. (C) Longitudinal gray scale ultrasound showing a normal fibrillar structure of the extensor tendons (red arrows) in a normal individual for comparison with (A). No increased power doppler was seen (not shown).



Figure 20 Tennis elbow with partial tear of the proximal extensor tendon in a 58-year-old tennis player. (A) Longitudinal ultrasound showing an anechoic defect at the deep side of the extensor tendon with subtle sparing of the superficial tendon fibers. (B) Axial. (C) Sagittal and (D) coronal FS T2-WI showing a fluid-filled defect in the proximal extensor tendons (arrows). FS, fat suppressed; WI, weighted image.

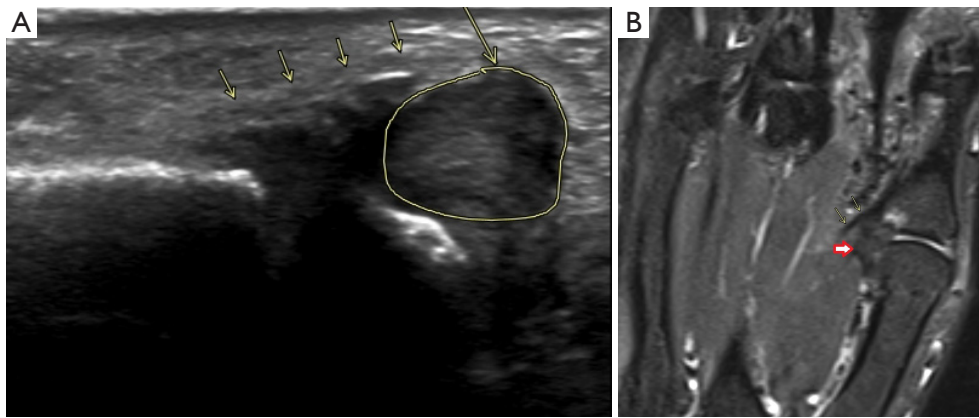


Figure 21 Stener lesion. (A) Longitudinal ultrasound in a 57-year-old female skier showing a yoyo (circle) on string (small arrows) corresponding to the retracted UCL and adductor aponeurosis respectively. (B) Coronal FS-T2-WI in another middle-aged skier shows a retracted and entrapped UCL (red arrows) proximal to the adductor aponeurosis (small arrows). Also note bone marrow edema at the ulnar side of the proximal phalanx. UCL, ulnar collateral ligament; FS, fat suppressed; WI, weighted image.

interposition of the adductor pollicis aponeurosis preventing healing (58).

Radiographs may detect avulsion fracture at the ulnar base of the proximal phalanx of the thumb. Stress radiographs may be useful for evaluation of metacarpophalangeal instability.

US and MRI are used to evaluate whether the tear is partial or complete, to assess the degree of retraction and whether a Stener lesion is present (58). MRI may show bone marrow edema at the site of avulsion at the proximal phalanx. In case of a Stener lesion, the proximal retracted interposed UCL will be seen as a yoyo on a string (*Figure 21*). Furthermore, US has the advantage to enable assessment of joint instability. The adductor aponeurosis will not slide freely over the UCL on passive thumb interphalangeal joint flexion if a Stener lesion is present (20).

The most important role for imaging is to document Stener lesion, joint instability, and displaced avulsion fractures, which are indications for surgical stabilization (59).

Conclusions

In our radiological practice, there is a steady increase of referrals for sports injuries in middle-aged and older patients. This may be due to several factors such as increased life expectancy and the fact that activity is promoted as having a positive effect on mental and physical well-being. *Table 1* summarizes the most common lesions and their key imaging characteristics, that may serve as a quick guideline for radiologists and referring physicians.

It is important to realize that a sport-related lesion in the elderly often occurs on a terrain on pre-existing tendinosis. Furthermore, because of the high prevalence of MSK lesions in older asymptomatic patients, imaging findings must be carefully correlated with the clinical presentation. The management of sports injuries in the elderly is often more conservative than in younger sporters. We acknowledge that the referral pattern of sport-related lesions in the aging population may differ from center to center related to local circumstances such as availability of imaging facilities, differences in referral guidelines for imaging in different

Table 1 Summary of the top 15 MSK lesions in recreational aging sporters, mechanism of trauma, preferred imaging technique and imaging signs

Lesion	Trauma mechanism	Preferred technique	Main imaging signs
Hamstrings rupture	Eccentric muscle contraction with flexed hip and extended knee	MRI > US	High T2 signal, discontinuity, retraction
Meniscal tear	Knee twisting (predominantly while the foot is planted on the ground)	MRI	Increased T2 signal communicating with free edge on 2 slices Abnormal shape and displacement of the meniscus
ACL lesion	Sudden pivoting maneuver	MRI	High T2 signal, discontinuity Secondary sign of BME lateral condyle and posterolateral tibia
Subchondral insufficiency fracture	Overload	MRI	Subchondral hypointense fracture line with surrounding BME
Stress fracture	Overload	MRI	Fracture line, BME, soft tissue edema
Tennis leg	Hyperextension of the knee with flexion of the foot	US	Partial or complete discontinuity of the distal myotendinous junction of the MG Fluid deep to the MG and superficial to soleus muscle
Achilles tendon pla, tear	Sudden contraction of gastrocnemius and soleus muscles	US (MRI for staging/preop cartography)	High T2 signal, discontinuity, retraction
Morton's fibroma	Entrapment of common digital plantar nerves	US/MRI	Mass between metatarsal heads, sonographic Mulder sign
Snowboard fracture ankle	Dorsiflexion and inversion of the ankle	CT/MRI	Fracture at the lateral process of the talus
Morel-Lavallée lesion	Shearing injury	US (MRI for extensive lesions)	Serosanguineous collection between subcutaneous fat and underlying fascia, intralesional fat globules
Rotator cuff tear	Acute (fall) trauma often with pre-existing tendon degeneration	US as initial examination. MR arthrography for size, extent, muscle status	Partial or full-thickness tendon defect. Atrophy and fatty infiltration of muscles in advanced cases
Distal clavicular osteolysis	Repetitive overhead microtrauma	MRI > CR > US	Irregular delineation of the articular side of the clavicle, widening AC joint, BME
Biceps brachii tendon rupture	Eccentric loading	US (MRI for staging/preop cartography)	High T2 signal, discontinuity, retraction
Tennis/golfers elbow	Valgus/varus overuse	US (MRI)	Tendinosis: thickening, hypoechogenicity, increased power doppler signal, Intermediate high T2-signal Tear: partial or full-thickness tendon defect, high T2 signal
Ulnar collateral ligament thumb	Thumb abduction	US (MRI)	Discontinuity, retraction (look for Stener lesion!)

MSK, musculoskeletal; MRI, magnetic resonance imaging; US, ultrasound; ACL, anterior cruciate ligament; BME, Boen Marrow Edema; MG, medial gastrocnemius; CR, conventional radiography; AC, acromioclavicular.

countries and different economic conditions in high-income countries versus low-income countries.

Acknowledgments

The author thanks Dr. Gunther De Praeter for his assistance in imaging reporting.

Funding: None.

Footnote

Provenance and Peer Review: With the arrangement by the Guest Editor and the editorial office, this article has been reviewed by external peers.

Conflicts of Interest: The author has completed the ICMJE uniform disclosure form (available at <https://qims.amegroups.com/article/view/10.21037/qims-22-1294/coif>). The special issue “Imaging of Aging and Age-Related Disorders” was commissioned by the editorial office without any funding or sponsorship. The author has no other conflicts of interest to declare.

Ethical Statement: The author is accountable for all aspects of the work in ensuring that questions related to the accuracy or integrity of any part of the work are appropriately investigated and resolved.

Open Access Statement: This is an Open Access article distributed in accordance with the Creative Commons Attribution-NonCommercial-NoDerivs 4.0 International License (CC BY-NC-ND 4.0), which permits the non-commercial replication and distribution of the article with the strict proviso that no changes or edits are made and the original work is properly cited (including links to both the formal publication through the relevant DOI and the license). See: <https://creativecommons.org/licenses/by-nc-nd/4.0/>.

References

- Jenkin CR, Eime RM, Westerbeek H, O'Sullivan G, van Uffelen JGZ. Sport and ageing: a systematic review of the determinants and trends of participation in sport for older adults. *BMC Public Health* 2017;17:976.
- Khan KM, Thompson AM, Blair SN, Sallis JF, Powell KE, Bull FC, Bauman AE. Sport and exercise as contributors to the health of nations. *Lancet* 2012;380:59-64.
- Masters RK, Woolf SH, Aron LY. Age-Specific Mortality During the 2020 COVID-19 Pandemic and Life Expectancy Changes in the United States and Peer Countries, 1980-2020. *J Gerontol B Psychol Sci Soc Sci* 2022;77:S127-37.
- D'Onofrio G, Kirschner J, Prather H, Goldman D, Rozanski A. Musculoskeletal exercise: Its role in promoting health and longevity. *Prog Cardiovasc Dis* 2023. doi: 10.1016/j.pcad.2023.02.006.
- Johnson J, von Stade D, Gadomski B, Regan D, Easley J, Sikes KJ, Troyer K, Zhou T, Schlegel T, McGilvray K. Biomechanical and histological changes secondary to aging in the human rotator cuff: A preliminary analysis. *J Orthop Res* 2023. doi: 10.1002/jor.25529
- Fuchs CJ, Kuipers R, Rombouts JA, Brouwers K, Schrauwen-Hinderling VB, Wildberger JE, Verdijk LB, van Loon LJC. Thigh muscles are more susceptible to age-related muscle loss when compared to lower leg and pelvic muscles. *Exp Gerontol* 2023;175:112159.
- Llopis E, Aparisi Gómez MP, Idoate F, Padron M. The aging athlete. In: Vanhoenacker F, Maas M, Gielen JLMA, editors. *Imaging of Orthopedic Sports Injuries*. Second edition. Cham: Springer Nature, 2021:723-52.
- Lefere M, Demeyere A, Vanhoenacker F. Overuse Bone Trauma and Stress Fractures. In: Vanhoenacker F, Maas M, Gielen JLMA, editors. *Imaging of Orthopedic Sports Injuries*. Second edition. Cham: Springer Nature, 2021:135-50.
- Karantanas AH. Natural History and Monitoring of Fractures and Microfractures. In: Vanhoenacker F, Maas M, Gielen JLMA, editors. *Imaging of Orthopedic Sports Injuries*. Second edition. Cham: Springer Nature, 2021:755-82.
- Neuschwander TB, Benke MT, Gerhardt MB. Anatomic Description of the Origin of the Proximal Hamstring. *Arthroscopy: the journal of arthroscopic & related surgery : official publication of the Arthroscopy Association of North America and the International Arthroscopy Association*. *Arthroscopy* 2015;31:1518-21.
- Mathew K, Pillarisetty LS. Anatomy, Bony Pelvis and Lower Limb: Thigh Semitendinosus Muscle. 2022 May 31. In: *StatPearls*. Treasure Island (FL): StatPearls Publishing, 2023.
- Sheean AJ, Arner JW, Bradley JP. Proximal Hamstring Tendon Injuries: Diagnosis and Management. *Arthroscopy* 2021;37:435-7.
- Bencardino JT, Mellado JM. Hamstring injuries of the hip. *Magn Reson Imaging Clin N Am* 2005;13:677-90, vi.
- Nguyen JC, De Smet AA, Graf BK, Rosas HG. MR

- imaging-based diagnosis and classification of meniscal tears. *Radiographics* 2014;34:981-99.
15. Mezhov V, Teichtahl AJ, Strasser R, Wluka AE, Cicuttini FM. Meniscal pathology - the evidence for treatment. *Arthritis Res Ther* 2014;16:206.
 16. Herrlin S, Hållander M, Wange P, Weidenhielm L, Werner S. Arthroscopic or conservative treatment of degenerative medial meniscal tears: a prospective randomised trial. *Knee Surg Sports Traumatol Arthrosc* 2007;15:393-401.
 17. Herrlin SV, Wange PO, Lapidus G, Hållander M, Werner S, Weidenhielm L. Is arthroscopic surgery beneficial in treating non-traumatic, degenerative medial meniscal tears? A five year follow-up. *Knee Surg Sports Traumatol Arthrosc* 2013;21:358-64.
 18. Thorlund JB, Juhl CB, Roos EM, Lohmander LS. Arthroscopic surgery for degenerative knee: systematic review and meta-analysis of benefits and harms. *Br J Sports Med* 2015;49:1229-35.
 19. Sanders TG, Medynski MA, Feller JF, Lawhorn KW. Bone contusion patterns of the knee at MR imaging: footprint of the mechanism of injury. *Radiographics* 2000;20 Spec No:S135-51.
 20. Palmer W, Bancroft L, Bonar F, Choi JA, Cotten A, Griffith JE, Robinson P, Pfirrmann CWA. Glossary of terms for musculoskeletal radiology. *Skeletal Radiol* 2020;49:1-33.
 21. Hussain ZB, Chahla J, Mandelbaum BR, Gomoll AH, LaPrade RF. The Role of Meniscal Tears in Spontaneous Osteonecrosis of the Knee: A Systematic Review of Suspected Etiology and a Call to Revisit Nomenclature. *Am J Sports Med* 2019;47:501-7.
 22. Ochi J, Nozaki T, Nimura A, Yamaguchi T, Kitamura N. Subchondral insufficiency fracture of the knee: review of current concepts and radiological differential diagnoses. *Jpn J Radiol* 2022;40:443-57.
 23. Nelson FR, Craig J, Francois H, Azuh O, Oyetakin-White P, King B. Subchondral insufficiency fractures and spontaneous osteonecrosis of the knee may not be related to osteoporosis. *Arch Osteoporos* 2014;9:194.
 24. Gorbachova T, Melenevsky Y, Cohen M, Cerniglia BW. Osteochondral Lesions of the Knee: Differentiating the Most Common Entities at MRI. *Radiographics* 2018;38:1478-95.
 25. Jose J, Pasquotti G, Smith MK, Gupta A, Lesniak BP, Kaplan LD. Subchondral insufficiency fractures of the knee: review of imaging findings. *Acta Radiol* 2015;56:714-9.
 26. Saragaglia D, Banihachemi JJ, Chamseddine AH. Acute injuries in Badminton from 10 to 66 years of age: an epidemiological study of 140 cases among all types of practice. *Eur J Orthop Surg Traumatol* 2023;33:1945-51.
 27. Delgado GJ, Chung CB, Lektrakul N, Azocar P, Botte MJ, Coria D, Bosch E, Resnick D. Tennis leg: clinical US study of 141 patients and anatomic investigation of four cadavers with MR imaging and US. *Radiology* 2002;224:112-9.
 28. Harwin JR, Richardson ML. "Tennis leg": gastrocnemius injury is a far more common cause than plantaris rupture. *Radiol Case Rep* 2017;12:120-3.
 29. Vallone G, Vittorio T. Complete Achilles tendon rupture after local infiltration of corticosteroids in the treatment of deep retrocalcaneal bursitis. *J Ultrasound* 2014;17:165-7.
 30. Weinfeld SB. Achilles tendon disorders. *Med Clin North Am* 2014;98:331-8.
 31. Calleja M, Connell DA. The Achilles tendon. *Semin Musculoskelet Radiol* 2010;14:307-22.
 32. Pass B, Robinson P, Ha A, Levine B, Yablon CM, Rowbotham E. The Achilles Tendon: Imaging Diagnoses and Image-Guided Interventions-AJR Expert Panel Narrative Review. *AJR Am J Roentgenol* 2022;219:355-68.
 33. Eken G, Misir A, Tangay C, Atici T, Demirhan N, Sener N. Effect of muscle atrophy and fatty infiltration on mid-term clinical, and functional outcomes after Achilles tendon repair. *Foot Ankle Surg* 2021;27:730-5.
 34. Lawrence DA, Rolen MF, Morshed KA, Moukaddam H. MRI of heel pain. *AJR Am J Roentgenol* 2013;200:845-55.
 35. Van Royen A, Shahabpour M, Al Jahed D, Abid W, Vanhoenacker F, De Maeseneer M. Injuries of the Ligaments and Tendons in Ankle and Foot. In: Vanhoenacker FM, Maas M, Gielen JLMA, editors. *Imaging of Orthopedic Sports Injuries*. Second Edi. Cham: Springer Nature; 2021. p. 511-56.
 36. Bohyn C, Flores DV, Murray T, Mohr B, Cresswell M. Imaging Review of Snowboard Injuries. *Semin Musculoskelet Radiol* 2022;26:54-68.
 37. Jibri Z, Mukherjee K, Kamath S, Mansour R. Frequently missed findings in acute ankle injury. *Semin Musculoskelet Radiol* 2013;17:416-28.
 38. Kirkpatrick DP, Hunter RE, Janes PC, Mastrangelo J, Nicholas RA. The snowboarder's foot and ankle. *Am J Sports Med* 1998;26:271-7.
 39. De Coninck T, Vanhoenacker F, Verstraete K. Imaging Features of Morel-Lavallée Lesions. *J Belg Soc Radiol* 2017;101:15.
 40. Chen X, Zhou G, Xue H, Wang R, Bird S, Sun D, Cui L. High-Resolution Ultrasound of the Forefoot and

- Common Pathologies. Diagnostics (Basel) 2022.
41. Quinn TJ, Jacobson JA, Craig JG, van Holsbeeck MT. Sonography of Morton's neuromas. *AJR Am J Roentgenol* 2000;174:1723-8.
 42. Torriani M, Kattapuram SV. Technical innovation. Dynamic sonography of the forefoot: The sonographic Mulder sign. *AJR Am J Roentgenol* 2003;180:1121-3.
 43. Zanetti M, Strehle JK, Kundert HP, Zollinger H, Hodler J. Morton neuroma: effect of MR imaging findings on diagnostic thinking and therapeutic decisions. *Radiology* 1999;213:583-8.
 44. Abdelwahab A, Ahuja N, Iyengar KP, Jain VK, Bakti N, Singh B. Traumatic rotator cuff tears - Current concepts in diagnosis and management. *J Clin Orthop Trauma* 2021;18:51-5.
 45. Pierce J, Anderson M. Update on Diagnostic Imaging of the Rotator Cuff. *Clin Sports Med* 2023;42:25-52.
 46. Li L, Dong J, Li Q, Dong J, Wang B, Zhou D, Liu F. MRA improves sensitivity than MRI for the articular-sided partial-thickness rotator cuff tears. *Sci Prog* 2021;104:368504211059976.
 47. Kassarian A, Llopis E, Palmer WE. Distal clavicular osteolysis: MR evidence for subchondral fracture. *Skeletal Radiol* 2007;36:17-22.
 48. Nevalainen MT, Ciccotti MG, Morrison WB, Zoga AC, Roedl JB. Distal clavicular osteolysis in adults: association with bench pressing intensity. *Skeletal Radiol* 2016;45:1473-9.
 49. Roedl JB, Nevalainen M, Gonzalez FM, Dodson CC, Morrison WB, Zoga AC. Frequency, imaging findings, risk factors, and long-term sequelae of distal clavicular osteolysis in young patients. *Skeletal Radiol* 2015;44:659-66.
 50. Beazley JC, Lawrence TM, Drew SJ, Modi CS. Distal Biceps and Triceps Injuries. *Open Orthop J* 2017;11:1364-72.
 51. Tamborrini G, Müller-Gerbl M, Vogel N, Haeni D. Ultrasound of the elbow with emphasis on the sonoanatomy of the distal biceps tendon and its importance for the surgical treatment of tendon lesions. *J Ultrason* 2020;20:e129-34.
 52. Miller TT, Adler RS. Sonography of tears of the distal biceps tendon. *AJR Am J Roentgenol* 2000;175:1081-6.
 53. Konin GP, Nazarian LN, Walz DM. US of the elbow: indications, technique, normal anatomy, and pathologic conditions. *Radiographics* 2013;33:E125-47.
 54. Chew ML, Giuffrè BM. Disorders of the distal biceps brachii tendon. *Radiographics* 2005;25:1227-37.
 55. Willaume T, Bierry G. Biceps, Brachialis, and Triceps. *Semin Musculoskelet Radiol* 2021;25:566-73.
 56. Levin D, Nazarian LN, Miller TT, O'Kane PL, Feld RI, Parker L, McShane JM. Lateral epicondylitis of the elbow: US findings. *Radiology* 2005;237:230-4.
 57. Walz DM, Newman JS, Konin GP, Ross G. Epicondylitis: pathogenesis, imaging, and treatment. *Radiographics* 2010;30:167-84.
 58. Rawat U, Pierce JL, Evans S, Chhabra AB, Nacey NC. High-Resolution MR Imaging and US Anatomy of the Thumb. *Radiographics* 2016;36:1701-16.
 59. Melville D, Jacobson JA, Haase S, Brandon C, Brigido MK, Fessell D. Ultrasound of displaced ulnar collateral ligament tears of the thumb: the Stener lesion revisited. *Skeletal Radiol* 2013;42:667-73.

Cite this article as: Vanhoenacker FM. Top 15 musculoskeletal lesions in the aging recreational sporter: a pictorial review. *Quant Imaging Med Surg* 2023;13(11):7552-7571. doi: 10.21037/qims-22-1294

Supplementary

Table S1 Pulse recommendations for routine imaging of the pelvis and hamstrings tendons

Pulse sequence	WI	Plane	No. of sections	TR (ms)	TE (ms)	Echo train length	Section thickness (mm)
FSE	T1	Coronal	28	643	12	3	4.4
FS FSE	PD	Coronal	28	3,080	47	5	4.4
FS FSE	PD	Axial	36	4,500	41	18	4
FS FSE	T2	Sagittal	40	9,200	53	15	2

WI, weighted image; TR, repetition time (ms); TE, echo time (ms); FSE, Fast Spin Echo; FS, fat suppressed.

Table S2 Pulse recommendations for the knee

Pulse sequence	WI	Plane	No. of sections	TR (ms)	TE (ms)	Echo train length	Section thickness (mm)
SE	T1	Sagittal	22	494	13	1	3,5
FS FSE	PD	Coronal	22	2,650	26	7	3
FS FSE	PD	Axial	22	3,090	43	5	3,5
FS FSE	PD	Sagittal	22	2,530	29	9	3,5

WI, weighted image; TR, repetition time (ms); TE, echo time (ms); SE, spin echo; FS, fat suppressed; FSE, Fast Spin Echo.

Table S3 Pulse recommendations for the ankle joint

Pulse sequence	WI	Plane	No. of sections	TR (ms)	TE (ms)	Echo train length	Section thickness (mm)
FSE	PD	Oblique coronal	25	3,090	25	9	3
FS FSE	PD	Oblique coronal	25	3,730	30	10	3
FS FSE	PD	Oblique axial	30	2,290	35	9	3.5
FS FSE	PD	Sagittal	24	4,890	33	10	3
FSE	T1	Oblique axial	30	650	12	3	3.5

WI, weighted image; TR, repetition time (ms); TE, echo time (ms); FSE, Fast Spin Echo; FS, fat suppressed.

Table S4 Pulse recommendations for the forefoot

Pulse sequence	WI	Plane	No. of sections	TR (ms)	TE (ms)	Echo train length	Section thickness (mm)
FS FSE	PD	Long axis	20	3,600	45	9	3
FS FSE	PD	Short axis	22	3,000	39	9	3
FSE	T1	Short axis	29	610	29	3	3
TIRM	T2	Sagittal	22	5,680	68	9	4
Optional (plantar plate; Morton) -/+gadolinium contrast	FST1	Short axis and sagittal	30	610	11	3	3

WI, weighted image; TR, repetition time (ms); TE, echo time (ms); FS, fat suppressed; FSE, Fast Spin Echo; TIRM turboIR with a Magnitude display.

Table S5 Pulse recommendations for MR arthrography of the shoulder following intra-articular injection of dilute gadolinium contrast

Pulse sequence	WI	Plane	No. of sections	TR (ms)	TE (ms)	Echo train length	Section thickness (mm)
FS FSE	PD	Oblique coronal	22	2,930	28	6	2.5
FS FSE	T1	Oblique sagittal	26	777	10	3	3
FS FSE	T1	Axial	30	755	8	3	2.1
FS FSE	T1	Oblique coronal	22	666	11	3	2.5
Optional (full thickness tear) FSE	T1	Oblique sagittal through muscle belly	24	488	11	3	3

WI, weighted image; TR, repetition time (ms); TE, echo time (ms); FS, fat suppressed; FSE, Fast Spin Echo.

Table S6 Pulse recommendations for the elbow

Pulse sequence	WI	Plane	No. of sections	TR (ms)	TE (ms)	Echo train length	Section thickness (mm)
FS FSE	PD	Oblique coronal	30	4,740	38	9	2.5
FS FSE	PD	Oblique sagittal	25	3,230	39	5	2.5
FS FSE	PD	Oblique axial	33	4,350	48	7	2.2
FSE	PD	Oblique coronal	20	642	11	2	3
FSE	T1	Oblique coronal	20	642	11	2	3
Optional (biceps) Dixon	T2	FABS	24	3,460	75	18	3

WI, weighted image; TR, repetition time (ms); TE, echo time (ms); FS, fat suppressed; FSE, Fast Spin Echo; FABS, Flexion Abduction Supination.

Table S7 Pulse recommendations for the thumb

Pulse sequence	WI	Plane	No. of sections	TR (ms)	TE (ms)	Echo train length	Section thickness (mm)
TrueFISP	T2*	3D	80	10.54	4.75	1	0.5
FS FSE	pd	Axial	20	3,100	36	9	2.5
FS FSE	pd	Oblique coronal	14	3,500	36	19	2
SE	T1	Oblique coronal	12	400	22	1	2

WI, weighted image; TR, repetition time (ms); TE, echo time (ms); FS, fat suppressed; FSE, Fast Spin Echo; TrueFISP, fast imaging with steady-state free precession; SE, spin echo.